Is antitumor Pt(IV) complex containing two axial lonidamine ligands a true dual- or multi-action prodrug?

Jana Kasparkova, Hana Kostrhunova, Vojtech Novohradsky, Lili Ma, Guangyu Zhu, Elena R Milaeva, Alexender A Shtill, Robin Vinck, Gilles Gasser, Viktor Brabec, et al.

Is antitumor Pt(IV) complex containing two axial lonidamine ligands a true dual- or multi-action prodrug?

Jana Kasparkova[1], Hana Kostrhunova[1], Vojtech Novohradsky[1], Lili Ma[2], Guangyu Zhu[2], Elena R. Milaeva[3], Alexender A. Shtill[4], Robin Vinck[5], Gilles Gasser[5], Viktor Brabec[1*] and Alexey A. Nazarov[3*]

1. *Czech Academy of Sciences, Institute of Biophysics, Brno CZ-61265, Czech Republic*
2. *Department of Chemistry, City University of Hong Kong, Hong Kong SAR, P. R. China*
3. *Lomonosov Moscow State University, Faculty of Chemistry, 119991 Moscow, Russian Federation*
4. *Blokhin Cancer Center, 115478 Moscow, Russian Federation*
5. *Chimie ParisTech, PSL University, CNRS, Institute of Chemistry for Life and Health Sciences, Laboratory for Inorganic Chemical Biology, 75005 Paris, France*

Correspondence should be addressed to Alexey A. Nazarov; nazarov@med.chem.msu.ru or Viktor Brabec; brabec@ibp.cz

Abstract

This work studied the mechanism of action of a Pt(IV) complex **2** bearing two axial lonidamine ligands, which are selective inhibitors of aerobic glycolysis. The presence of two lonidamine ligands in **2** compared to the parent Pt(II) complex increased its antiproliferative activity, cellular accumulation, and changed its cell cycle profile and mechanism of cell death. In 3D cell culture, **2** showed exceptional antiproliferative activity with IC50 values as low as 1.6μM in MCF7 cells. The study on the influence of the lonidamine ligands in the Pt complex on glycolysis showed only low potency of ligands to affect metabolic processes in cancer cells, making the investigated complex, not a dual- or multi-action prodrug. However, the Pt(IV) prodrug effectively delivers cytotoxic Pt(II) complex into cancer cells.

Keywords: Bioinorganic Chemistry, Lonidamine, Medicinal Inorganic Chemistry Metals in Medicine Pt(IV) complexes

Introduction

Platinum(II) drugs are the current gold standard in cancer chemotherapy.[1-4] Currently, we have a good understanding of cell transport and mechanism of action of platinum drugs, possible side effects, and resistant phenomena.[5-10] To overcome some limitations and side effects of conventional Pt(II) antitumor drugs, Pt(IV) prodrugs are attracting considerable interest, mostly due to reduced general toxicity, the possibility for oral administration, and red-ox kinetics as part of the mechanism of action.[11-14] Additionally, Pt(IV)-based prodrugs have the potential of combining several bioactive moieties in a single molecule releasing the FDA-approved Pt(II) drugs, cisplatin, carboplatin, or oxaliplatin, together with other antiproliferative agents. Several Pt(IV) drug candidates have been investigated in the clinical trials; however, none has been approved as an anticancer drug. The current shift of interest in anticancer Pt(IV) complexes is to modify axial position(s) with innocent spectators, cancer-targeting agents, photodynamic therapy photosensitizers, or bioactive moieties to increase antitumor efficacy and/or overcome resistance.[15-24] Upon entering the cell, Pt(IV) prodrugs can be reduced by intracellular reductants to generate DNA-damaging Pt(II) drugs. Simultaneously, bioactive axial moieties are released inside the cancer cells, resulting in a combined effect that triggers several processes, which determine the cell's fate. Thus, Pt(IV) complexes are often dual or multi-action drugs that can increase the efficacy and/or overcome resistance to conventional Pt(II) anticancer drugs. On

the other hand, markedly enhanced accumulation of Pt(IV) prodrugs due to their hydrophobic character has been shown to play a key role in the markedly enhanced antitumor activity of several Pt(IV) derivatives of conventional antitumor Pt(II) drugs with bioactive ligands.[25-27]

Lonidamine (**1**, Figure 1) is a selective inhibitor of aerobic glycolysis in cancer cells[28-30] and was evaluated in clinical trials as monotherapy or combination therapy against lung, prostate, breast, and non-small cell lung cancer.[28, 31-33] Additionally, lonidamine is commonly used as a chemosensitizer to enhance the antitumor effects of chemotherapeutic drugs based on its disruption of energy metabolism.[34, 35] Several Pt(IV) complexes with lonidamine were prepared to target mitochondrial pathways.[22, 36, 37] Moreover, tethering of lonidamine to Ru(II)-arene moiety yields compounds with highly relevant cytotoxicity in human glioblastoma cell lines.[38] Recently, we reported on the new highly active Pt(IV) complexes with lonidamine as axial ligands.[39, 40] We found that conjugation with lonidamine resulted in compounds with superior activity compared to the original organic drug, but also cisplatin. Out of all prepared complexes, we selected the most active one, namely (OC-6–33)-dichloridobis[1-(2,4-dichlorobenzyl)-1H-indazole-3-carboxylato](ethane-1,2-diamine)platinum(IV) (**2** Figure 1), i.e., Pt(IV) derivative of direct and simple analog of cisplatin dichlorido(ethane-1,2-diamine)platinum(II)with lonidamine at both axial positions,[39] to investigate the mechanism underlying the antiproliferative effects of this prodrug in cancer cells. We were particularly interested in investigating the contribution of platinum and lonidamine to killing cancer cells cultured in traditional two-dimensional (2D) monolayers and three-dimensional (3D) spheroids.

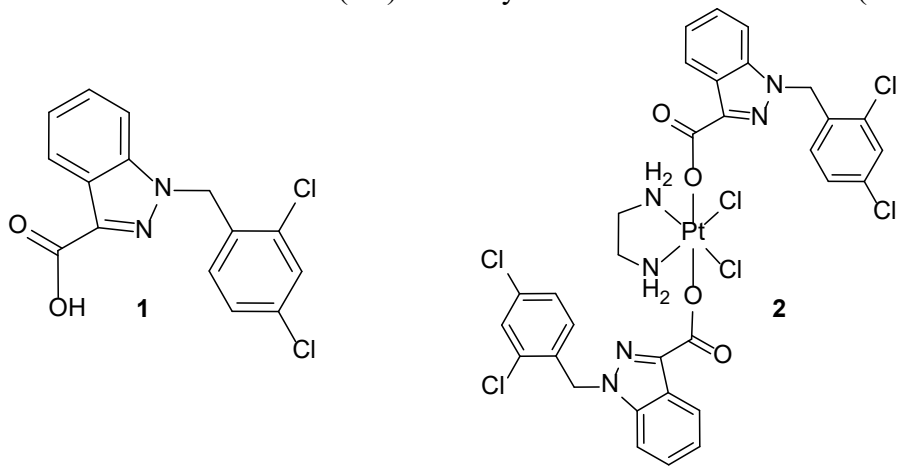

Figure 1. Structures of lonidamine (**1**) and (OC-6–33)-dichloridobis[1-(2,4-dichlorobenzyl)-1H-indazole-3-carboxylato](ethane-1,2-diamine)platinum(IV) (**2**).

Results and Discussion

Synthesis

1-(2,4-Dichlorobenzyl)-1H-indazole-3-carboxylic acid (Lonidamine (**1**))[41] and (OC-6–33)-dichloridobis[1-(2,4-dichlorobenzyl)-1H-indazole-3-carboxylato](ethane-1,2-diamine)platinum(IV) (**2**)[39] were prepared using published procedures. Compounds were characterized using ^{1}H NMR and mass spectrometry and were fully identical to the described in the literature.[39] The purity of prepared compounds was established by combustion analysis.

Antiproliferative activity

The first prerequisite for using the investigated potential antitumor substances as effective chemotherapeutics is their sufficient antiproliferative activity in cancer cell lines. Successful antitumor chemotherapeutics should eliminate the expansion of solid tumor mass and/or indispose cancer cells in cell division.

Antiproliferative activity of complex **2** was studied by the commonly used MTT assay after 72 h of incubation on three human cancer cell lines of different origin cultured in 2D monolayers; breast cancer MCF-7 cells, highly invasive, triple-negative breast carcinoma MDA-MB-231 cells, and colorectal carcinoma cells HCT-116 (Table 1). Moreover, the human noncancerous lung fibroblasts MRC-5pd30 were also included in the study. For comparative purposes, identical tests were performed with the clinically approved platinum(II) anticancer drug, cisplatin.

The data revealed that complex **2** showed potency in the submicromolar scale (Table 1). Notably, **2** displayed 20 - to 78-fold greater potency than clinically approved cisplatin. In addition, the experiments also confirm significantly (ca. 5-6-fold) lower activity in noncancerous skin fibroblasts, thus indicating selectivity for cancer over noncancerous human cells. Antiproliferative activity of free lonidamine was considerably lower than the activity of **2** or cisplatin (328 – 379-fold or 20 – 78-fold, respectively).

The MTT assay is dependent on mitochondrial respiration, specifically on the reduction of MTT to formazan catalyzed by mitochondrial succinate dehydrogenase.[42] Thus, some test compounds capable of affecting mitochondrial function may interfere with the conversion of the dye to colored formazan so that the MTT assay may yield false results. Platinum(IV) complex **2** contains lonidamine which has been known to inhibit aerobic glycolysis in cancer cells by inhibiting the mitochondrially bound hexokinase.[43] Thus, it is a different enzyme than the one exploited in the MTT assay. However, to make sure that the results obtained using the MTT assay are not affected by the effect of lonidamine on mitochondria, we also used another assay for quantitative estimation of the number of viable cells in a culture based on the mechanism not associated with mitochondria, namely the neutral red (NR) uptake assay. This assay is based on the ability of viable cells to incorporate and bind the supravital dye neutral red in the lysosomes.[44] The results obtained using this assay showed that the IC_{50} values determined for **2** and cisplatin in MCF-7 cells did not differ significantly from those obtained by the MTT assay (Table 2).

To emphasize the possibility that the new antitumor compounds might be promising candidates for clinical testing and to improve the relevance of our *in vitro* results, we used 3D cell cultures (spheroids), which are much better at replicating *in vivo* environment than traditional 2D cultures. Cells grow in complex 3D cultures with heterogeneous regions, nutrient and oxygen gradients, intercellular and cell-extracellular matrix interactions, closely reflecting the tumor microenvironment.[45] Hence, 3D growth of immortalized established cell lines or primary cell cultures is regarded as a more stringent and representative model for performing *in vitro* drug screening.https://www.nature.com/articles/srep19103 - ref6[45-47] 3D cell cultures possess several important *in vivo* features of tumors such as cell-cell interaction,[48] hypoxia,[49] drug penetration,[50] response and resistance,https://www.nature.com/articles/srep19103 - ref9[49] and production/deposition of the extracellular matrix.[51] Last but not least, authentic 3D cell culture models using human cells can circumvent the drawbacks of animal models that, aside from the high cost and ethical considerations, are not always able to recapitulate human diseases or capture the side effect of drugs accurately. Also, several features of the *in vivo* solid tumors have been exhibited by tumor spheroids. The similarities in the drug responsiveness among the tumor spheroids and the animal models might largely be due to their similarities in enhanced cellular interactions via adhesion and secretion of soluble factors of tumors that lead to the low pH and hypoxia.[52]

Therefore, we also assessed the ability of complex **2** to inhibit 3D spheroid formation from MCF-7 cells known to reproducibly form spheroids,[53] under 3D cell culture conditions (Table 3). The 3D spheroids were cultured for 96 h to grow up to a tissue mass of around 200 μm in diameter, as described in the Experimental Section. The cells were then treated with various concentrations of **2** for an additional 72 h. The CellTiter-Glo 3D cell viability assay was used to determine IC_{50} values. The results (Table 3) confirmed that **2**, which is a very active drug in conventional 2D cell cultures (Table 1), exhibited exceptional activity also in the 3D spheroids formed from MCF- cells, being ~11-fold more effective than clinically used cisplatin.

The effect on the morphology of 3D spheroids formed from the suspension of MCF-7 single cells is shown in Figure 2. Spheroids formed by the control, untreated cells were of round-shape morphology with a well-defined surrounding edge (Figure 2, panel A). However, spheroids generated after the treatment with **2** (Figure 2, panels D-F) displayed heterogeneous morphology with a high number of dissociated cell clumps. Furthermore, these dissociated cell clumps were found to a greater extent than in the samples treated with cisplatin (Figure 2, panels B,C). Therefore, this microscopic study showed superior activity of **2** in the 3D spheroids formed from breast cancer MCF-7 cells.

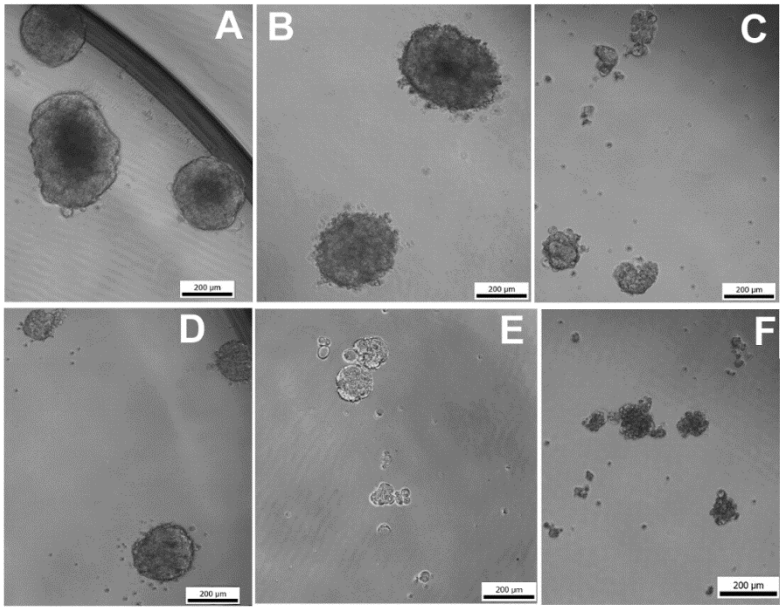

Figure 2. Representative bright-field images of 3D spheroids formed from MCF-7 cells untreated or treated with **2** or cisplatin. The 3D spheroids were cultured for 96 h to grow up to a tissue mass of around 200 µm in diameter, as described in the Experimental Section. The cells were further treated with the Pt complexes, and shots were taken after 72 h. Panels: A, control, untreated spheroids; B and C, the spheroids treated with cisplatin at 4 and 30 µM concentrations, respectively; D, E, and F, the spheroids treated with **2** at its 1, 4, and 7 µM concentration, respectively. Scale bars represent 200 µm.

Cellular accumulation

Cellular accumulation plays a fundamental role in the antiproliferative activity of low-molecular-mass compounds, including platinum complexes. It is so because cellular uptake or efflux belong to the initial steps in the mechanism of their antitumor effects.[9, 12] Therefore, we examined first how **2** accumulates in cancer cells. MCF-7 cells were treated with 10 µM **2** or cisplatin for 6 h, and the amount of platinum in cells was determined by ICP-MS. Platinum from **2** was taken up by the MCF-7 cells ca. 11-fold more efficiently than platinum from cisplatin (Table 4).

It was shown for several Pt(IV) complexes that they are transported into cells by passive diffusion dependent on their lipophilicity. [55, 56] However, it cannot be excluded that the involvement of active and facilitated transport mechanisms in the cellular accumulation of the investigated complex **2** can also affect their final cellular accumulation.[55] Therefore, we also examined whether the cellular uptake of **2** correlates with its lipophilic properties (log *P)*. The log *P* value for **2** determined previously[39] was positive (the compounds are lipophilic). Contrastingly, cisplatin itself is hydrophilic (log *P* = -2.3),[54] A clear correlation between the complex lipophilicity and cellular accumulation (Table 4) confirmed an assumption that hydrophobic rather than hydrophilic platinum compound penetrates the cytoplasmic membrane more effectively. This supports the hypothesis that **2** is transported into cells by passive diffusion, although the involvement of active and facilitated transport mechanisms cannot be excluded. The data also revealed that the enhanced cellular accumulation of platinum from the more hydrophobic

2 significantly contributes to its increased antiproliferative activity in MCF-7 cells compared with hydrophilic cisplatin. Moreover, an important implication of the marked differences between the cellular accumulation of platinum from **2** and cisplatin is that a significant part of the molecules of **2** enters the cells intact without being reduced already in the extracellular milieu of cultured cells.

Cell cycle profiles of MCF-7 cells

To further examine the mechanism(s) of action (MoA) of **2**, we investigated the cell-cycle profiles of MCF-7 cells treated with the investigated complex **2**. The cells were treated with various concentrations of **2** for 24 h (Figure 3). The cycle distribution of MCF-7 cells treated with **2** was analyzed by flow cytometry with untreated cells and cisplatin-treated cells as controls. As shown in Figure 3, exposure to a sublethal dose of cisplatin resulted in the accumulation of cells mainly in the S phase and slightly also in the G2/M phase. After treatment with **2**, the cells were also primarily arrested in S-phase, similarly to cisplatin. However, the percentage of cells accumulated in the S phase increased significantly compared to the effect of cisplatin. In contrast, the number of cells arrested in the G2/M phase remained unchanged compared to the control. Thus, the impact of **2** on the cell cycle resembles, to some extent, the parental cisplatin, supporting the view that the **2** acts via an overall mechanism similar to that of cisplatin.

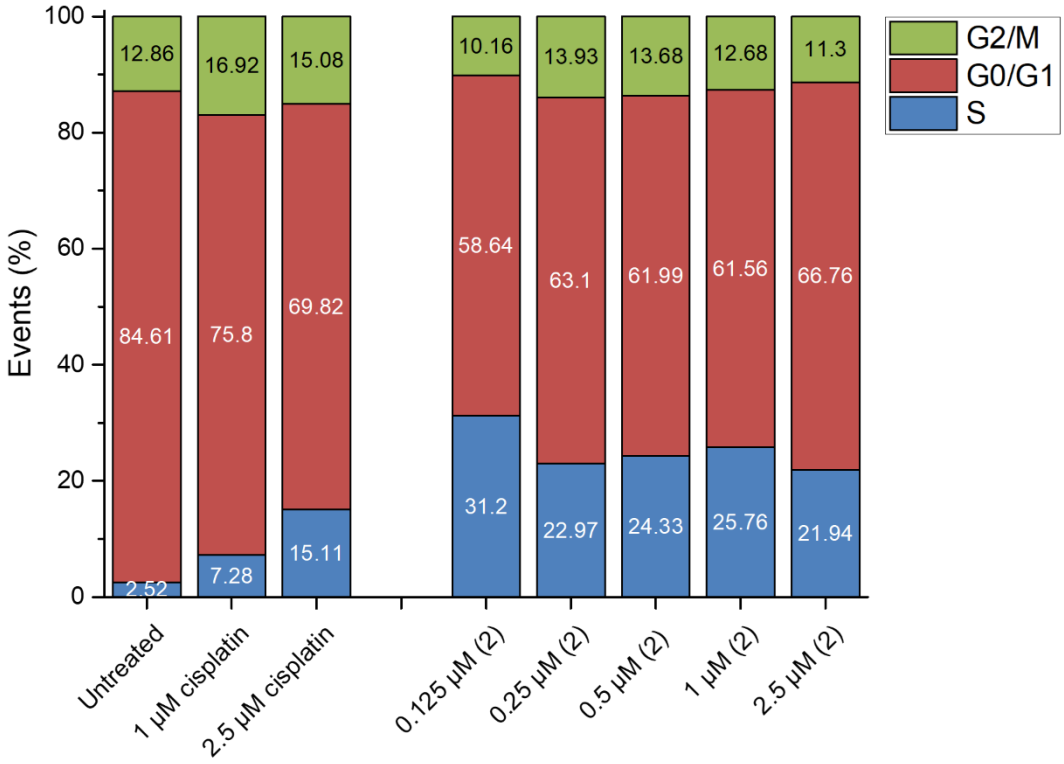

Figure 3. Cell cycle distribution of MCF-7 cells untreated or treated for 24 h at concentrations indicated in the Figure. The experiment was performed three times, and the results are expressed as mean.

Nature of cell death

Cell-based assays, such as the MTT assay, cannot distinguish between the cytostatic and cytotoxic effects of the investigated agents.[57] Therefore, we also investigated whether the treatment of MCF-7 cells with **2** can induce cell death and studied the mechanism of cell death. The levels of apoptosis and necrosis induced in MCF-7 cells by **2** or cisplatin at various concentrations over 12 h exposure time were quantified by the assay employing FITC Annexin V with 7-amino-actinomycin D (7-AAD) for the identification of apoptotic and necrotic cells by flow cytometry. The results demonstrated that **2** induced a 7.46 % fraction of early apoptosis at 0.25 μM, and the

ratio increased to 10.64% at 0.5 μM treatment. In addition, **2** showed a comparable fraction of late necrosis and late apoptosis compared to cisplatin. The results indicated apoptosis as a predominant mode of cell death; however, the effect of **2** was much more pronounced than that of cisplatin (Figure 4). These findings suggest that the nature of cell death induced in cancer cells by cisplatin and **2** was very similar or even identical. Thus, one can envision scenarios in which the mechanism of the antiproliferative effect of complex **2** is determined mainly by the impact of its platinum moiety.

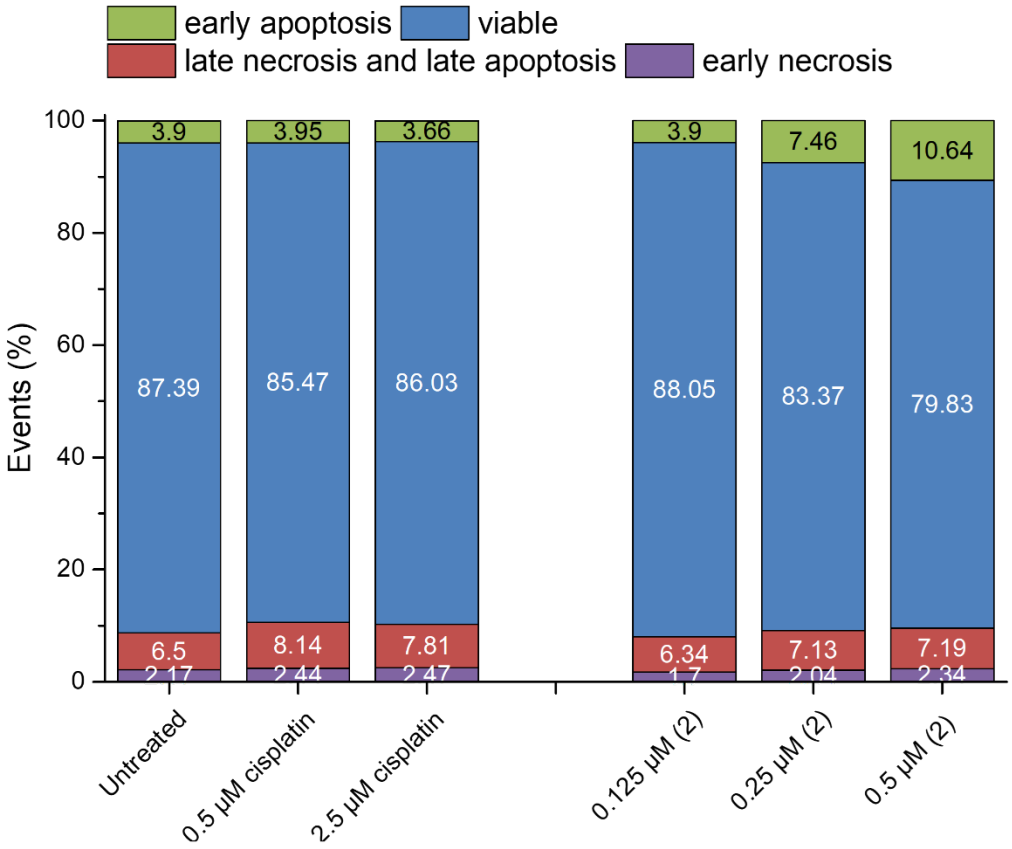

Figure 4. Effects of **2** and cisplatin on activation of the apoptotic and necrotic pathways in MCF-7 cells determined by the assay employing FITC Annexin V with 7-AAD by flow cytometry. Cells were treated for 12 h with **2** or cisplatin at the concentrations indicated in the figure. The results are expressed as the mean of two independent experiments with duplicate runs.

DNA platination and effect of DNA repair on the toxic effects of 2 in cancer cells *in vitro*

The important pharmacological target of cisplatin and its antitumor derivatives, including Pt(IV) prodrugs such as that examined in the present work, is nuclear DNA.[9] Cisplatin and its antitumor derivatives function in part through coordinative binding to DNA to form adducts that induce unique specific cellular responses, mainly culminating in apoptosis induction in cancer cells. Therefore, we further investigated whether the treatment of MCF-7 cells with **2** can result in the coordinative platination of nuclear DNA. The platination of DNA in MCF-7 cells treated with **2** was examined under experimental conditions identical to those used in the cellular uptake experiments (Table 4) using ICP-MS. The results (Table 5) show that under these experimental conditions, 15 picograms of platinum were associated with one microgram of DNA. This result insinuates that at least a part of **2** was reduced, releasing Pt(II) complex capable of coordinative binding to DNA because Pt(IV) complexes are substitution inert.

Nonetheless, to further explore whether DNA damage caused by the binding of platinum from **2** is involved in the mechanism of its antiproliferative activity, we performed an experiment to determine if DNA is an important target also for **2,** as is the case with other Pt(IV) complexes

derived from cisplatin-containing bioactive axial ligands.[56, 58-63] The target may be defined as a molecule whose alteration leads to cell death. One of the criteria used to suggest that DNA is the target is based on the observation that the drug exhibits higher toxicity in cells that are deficient in DNA repair [9] because the persistence and toxicity of DNA lesions depend on the capacity of cells to repair the damage. Therefore, the pair of Chinese hamster ovary CHO-K1 cell line (wild-type) and its mutant line MMC-2 [nucleotide excision repair (NER)-deficient, carrying the ERCC3/XPB mutation] was used to distinguish whether NER-reparable DNA damage induced by **2** is involved in the mechanism of action.

Cisplatin is believed to manifest its activity at least partially by damaging DNA,[9, 12] so it was not surprising that also in accord with the previously published data,[56] we found (Table 5) that cisplatin was ca. 11-fold more efficient in inhibiting proliferation of MMC-2 than CHO-K1 cells. Similarly, **2** was 9.4-fold more efficient in inhibiting proliferation of MMC-2 than CHO-K1 cells (Table 5), indicating that reparable DNA damage by platinum moiety released from **2** contributes significantly to the resulting biological activity.

Effect of 2 on glycolysis in cancer cells

To further explore the role of lonidamine ligands in the platinum(IV) prodrug **2** in the mechanism of its antiproliferative activity, we examined the effectiveness of **2** in inhibiting aerobic glycolysis in MCF-7 cancer cells. We opted for this study because **2** contains lonidamine, which is known to inhibit aerobic glycolysis in cancer cells by inhibiting the mitochondrially bound hexokinase.[43] Aerobic glycolysis is less efficient from an energetic standpoint than oxidative phosphorylation; therefore, cancer cells need to uptake more glucose to meet energy requirements. Moreover, lactate is produced and secreted to the microenvironment to maintain the cellular environment homeostasis.[64] Therefore, the effectiveness of **2** in inhibiting aerobic glycolysis in MCF-7 cancer cells was assessed by measuring the level of cellular glucose metabolism and lactate production using Amplex® Red Glucose/Glucose Oxidase Assay Kit (Life Technologies).

As expected, treatment of MCF-7 cells with free lonidamine for 24 h resulted in significantly ($P < 0.02$) lower glucose consumption compared with the untreated control or cells treated with cisplatin (Figure 5A). Interestingly, the effect of **2** was markedly less pronounced than that of free lonidamine at equitoxic concentrations. The slight decrease in glucose consumption was observed only at a relatively high concentration of **2**, corresponding to 3 times the IC_{50}; however, this effect was above the level of statistical significance ($p = 0.07$). Similarly, the effect of **2** on the level of lactate excreted after 6 h of incubation with **2** was low and insignificant (Figure 5B), even at very high concentrations (corresponding to 5 IC_{50}). In contrast, free lonidamine decreased lactate excretion significantly under the same conditions.

The data indicate that lonidamine ligands in axial positions of **2** were much less sufficient in shifting the cellular metabolism from glycolysis than free lonidamine, although they both induced the same antiproliferative effects (equitoxic concentrations were used). Thus, the observations that the effectiveness of **2** in inhibiting aerobic glycolysis in MCF-7 cancer cells is very low demonstrate that lonidamine ligands in **2** are functionally of only minor importance in the mechanism of its antiproliferative activity in cancer cells.

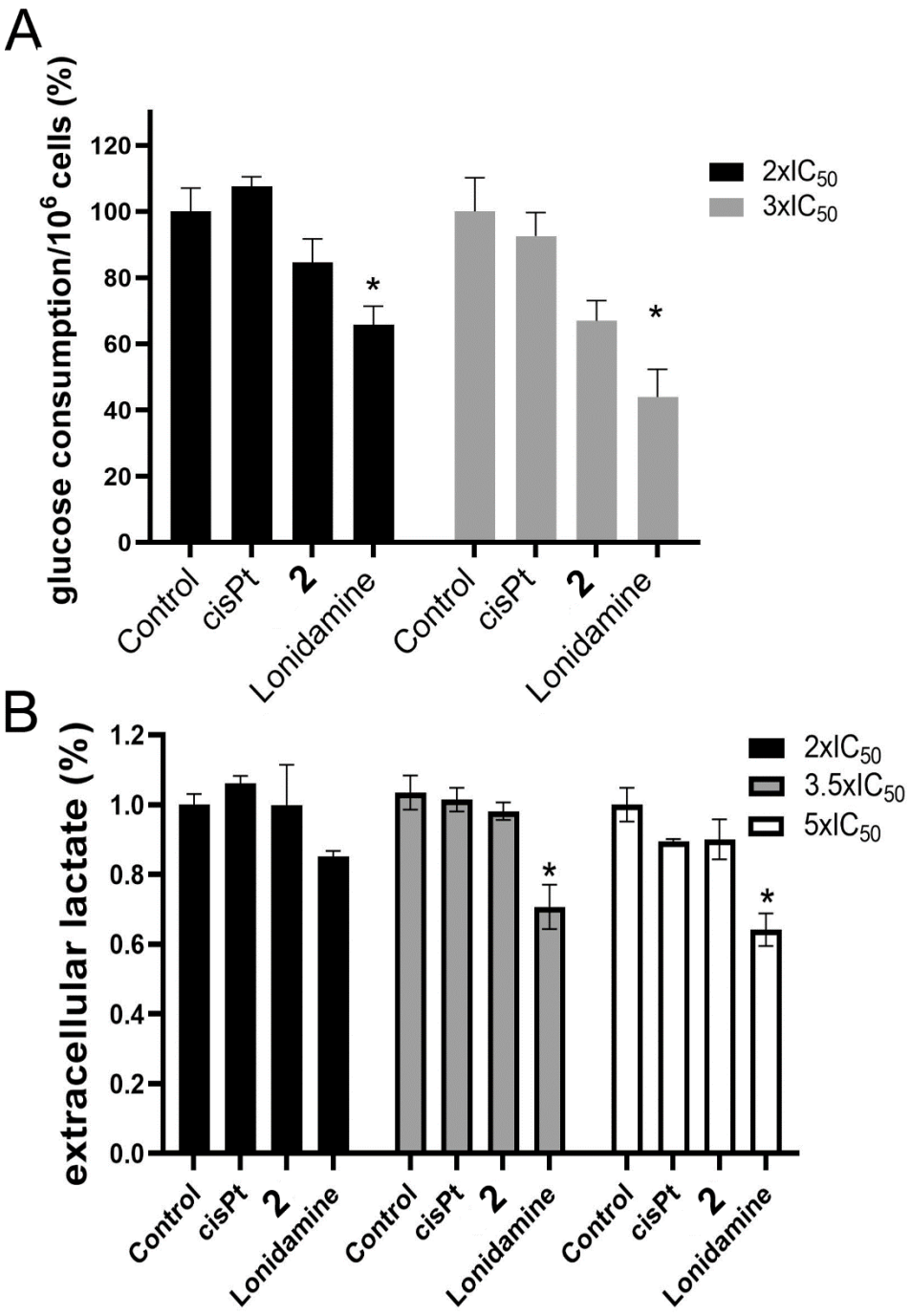

Figure 5: (A) Glucose consumption by MCF-7 cells as affected by **2**, cisplatin, and free lonidamime after 24 h of treatment at the indicated equitoxic concentrations. The amount of glucose taken up to the control, untreated cells was taken as 100%. (B) Modulation of extracellular lactate level in MCF-7cells after 6-h treatment with **2**, cisplatin, or free lonidamine at the concentrations indicated in the graph. The lactate level in the medium containing untreated control cells was taken as 100%. Figures A and B represent a mean ± SEM from three independent experiments. Stars indicate a difference from control, untreated cells (t-test): * $p < 0.05$.

These results were further confirmed by a glycostress test performed on MCF-7 cells using a Seahorse XF Analyzer. In this assay, subtle variations of the extracellular acidification rate (ECAR), which results from glucose consumption, can be followed in real-time while cells are subjected to different inhibitors injected in the medium. Each inhibitor shuts down or activates a metabolic pathway, allowing to probe how the metabolism of cells is affected by test compounds. For example, oligomycin inhibits mitochondrial respiration resulting in a metabolic shift towards glycolysis. In normal conditions, the oligomycin injection is therefore expected to be followed by

a sharp increase in the ECAR (Figure 6B). While this was the case with untreated cells or cells treated with 50 µM of **2** or cisplatin, no increase in the ECAR was observed when cells were pre-treated with 100 µM of lonidamine, indicating a severely impaired glycolytic capacity and glycolytic reserve (Figure 6A,C). These results, therefore, confirm that the lonidamine ligands in **2** do not inhibit glycolysis to the same extent as free lonidamine.

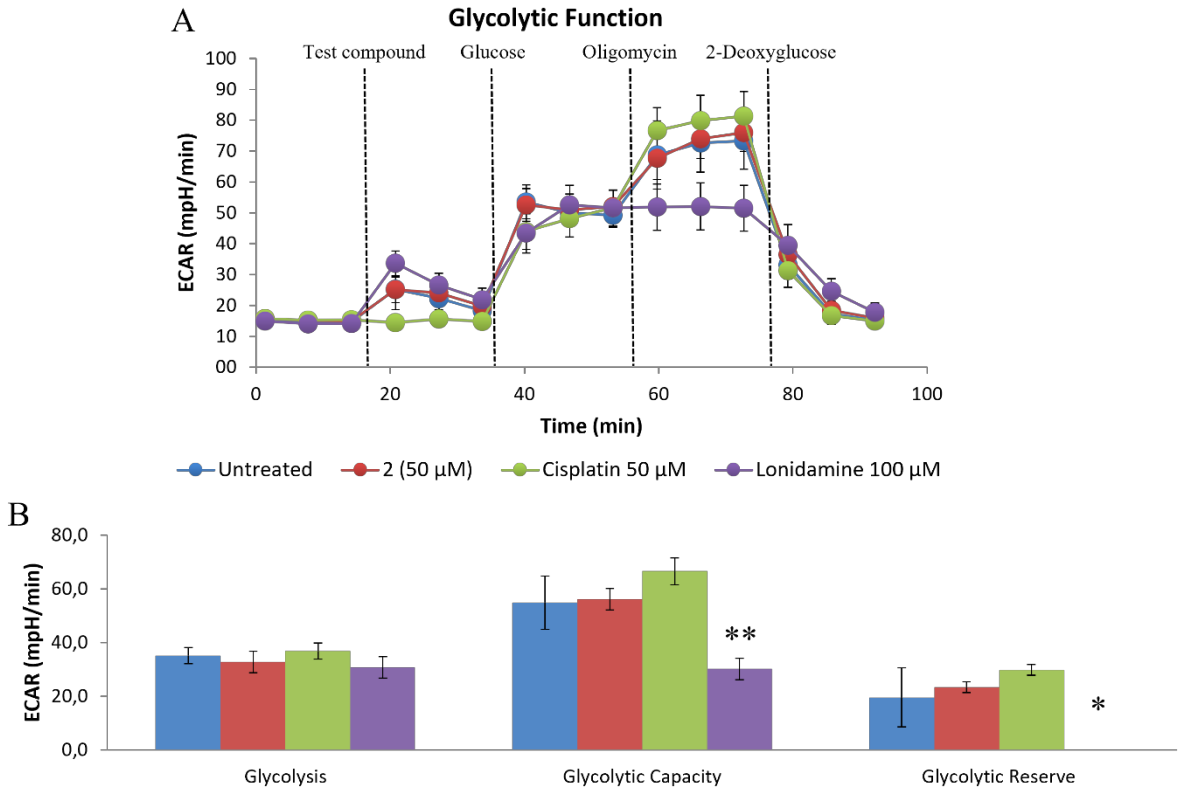

Figure 6: (A) Real-time Extracellular Acidification Rate (ECAR) as affected by the test compounds (**2**, cisplatin and lonidamine), followed by the injection of glucose, the mitochondrial respiration inhibitor oligomycin, and the glycolysis inhibitor 2-deoxyglucose in the medium as indicated by dashed lines. Only lonidamine prevented cells from switching their metabolism toward glycolysis when treated with oligomycin. (B) Effect of test compounds on the glycolytic parameters measured by the seahorse XFe Analyzer. Results presented as mean ± SD obtained using at least 8 replicate wells. Stars indicate a difference from untreated cells (t-test): * $p < 0.001$, ** $p < 0.0001$.

Effect of 2 on the level of glutathione in cancer cells.

In addition to the glycolysis inhibition, lonidamine was shown to affect many other metabolic processes in cancer cells.[29] Among them, reducing cellular levels of glutathione (GSH) is particularly important, as GSH interactions of platinum-based drugs lead to the elimination of Pt-drugs from cells and contribute to the resistance of cancer cells.[65] Thus, a decrease of intracellular concentration of GSH by lonidamine ligands from **2** should potentiate the activity of Pt moiety of **2**, resulting in a synergistic increase of activity. The level of GSH was then measured in MCF-7 cells treated with **2**, cisplatin, and free lonidamine at various concentrations and incubation periods. Monochlorobimane, a cell-permeant probe for quantifying glutathione levels in cells, was utilized for this experiment. To eliminate the possible impact of the presence of dead or damaged cells on the resulting data, we took advantage of flow cytometry, and the signals arising from potentially damaged cells were gated out.

The results shown in Figure 6 revealed that the level of GSH in cells was significantly elevated as a result of treatment with free lonidamine (except for the lowest concentration at 24 and 48 h of

treatment). In contrast, **2** was markedly less effective in increasing glutathione concentration, with provable effect only after a relatively long time of incubation (72 h)

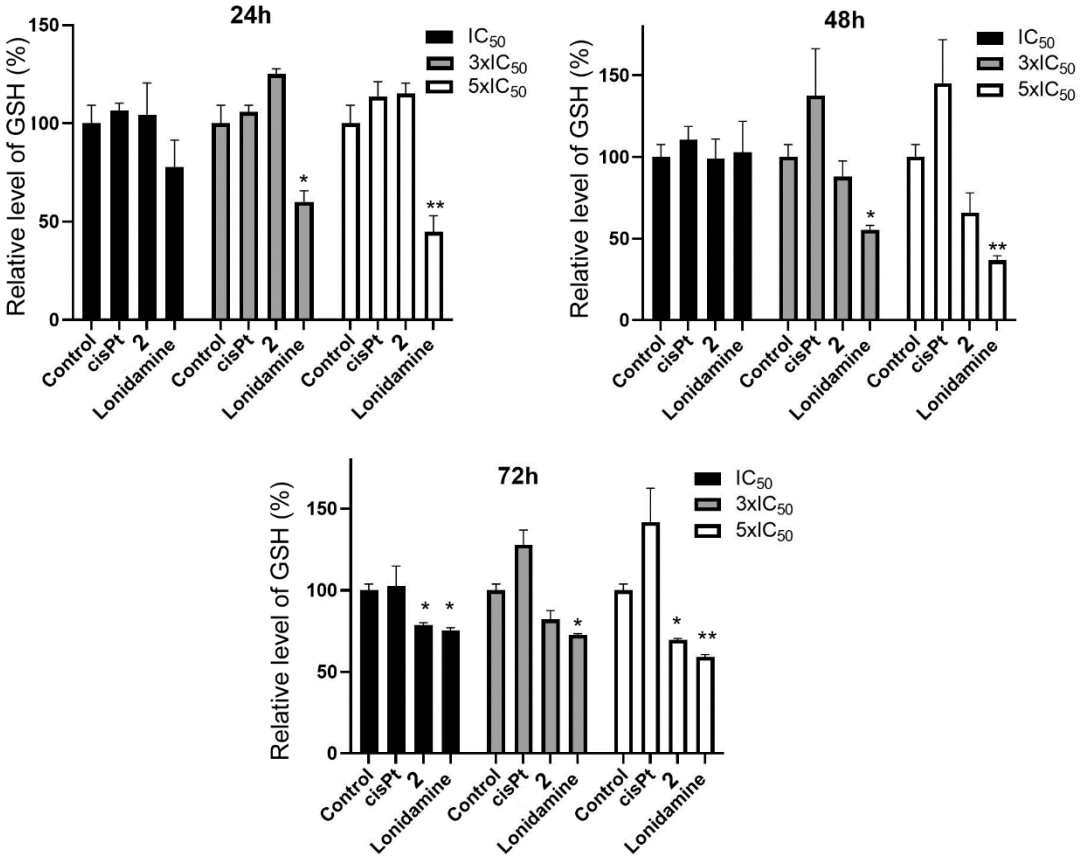

Figure 7: Levels of GSH determined in MCF-7 cells by flow cytometry. The cells were treated with equitoxic concentrations of the investigated compounds corresponding to 1-, 3-, or 5-fold $IC_{50,72h}$ and incubated for 24, 48, or 72 h. The median of the fluorescence of the treated samples was normalized to the untreated control level. Results are expressed as the mean ± SEM; stars indicate the difference from the untreated control: * $p<0.1$; ** $p< 0.05$

The low efficiency of **2** in increasing GSH concentration in cancer cells (Figure 7) is consistent with the data demonstrating the low effectiveness of **2** in inhibiting aerobic glycolysis in MCF-7 cancer cells (Figures 5A,B). These results indicate that two of the important functionalities of lonidamine, which affect metabolic processes in cancer cells, are unlikely to substantially contribute to the overall antiproliferative activity of **2** via their inherent biological activity; the effect of lonidamine ligands in **2** rather consists in the increase of accumulation of DNA damaging Pt moiety in cancer cells due to the elevated lipophilicity of **2**.

Tolerance of 2 *in vivo* and organ distribution

Finally, we tested the acute toxicity of complex **2** in Balb/c mice after a single bolus i.p. injection of the compound dissolved in saline. The doses were 70-125 mg/kg; higher doses were not achievable due to limited water solubility. Animals were monitored for 21 days after injection. No deaths were detected after injections of 125 mg/kg or 70 mg/kg. Mice in these cohorts had normal hair cover; no changes in nutritional behavior were registered over the entire period of observation. Biodistribution of **2** was studied in Balb/c mice using ICP-MS analysis of the platinum content in individual tissues. Compound **2** was injected i.p. at 75 mg/kg single bolus administration. The liver, kidney, lung, brain, and blood were collected after 24 h. This period is sufficient for a pilot judgment about drug distribution. Blood samples were separated into the plasma and cellular

fractions by centrifugation. As shown in Table 6, accumulation of **2** mostly in the liver and in the kidney, followed by lung and blood. As expected, complex **2** weakly penetrated the blood-brain barrier.

Conclusions

A Pt(IV) derivative of a direct and simple analog of cisplatin [*cis*-ethane-1,2-diaminedichloridoplatinum(II)] with lonidamine at both axial positions (complex **2**) was prepared and characterized by physicochemical methods. The investigated Pt(IV) complex showed exceptional antiproliferative activity in cancer cells cultured in 2D monolayers or contained in 3D spheroids (Tables 1 and 3). Complex **2** also displayed selectivity for cancer over noncancerous human cells. Additionally, our data indicate that platinum from **2** was taken up by the cancer cells markedly more efficiently than platinum from cisplatin, apparently due to the higher hydrophobicity of **2**. An important implication of the marked differences between the cellular accumulation of platinum from **2** and cisplatin is that a significant part of the **2** enters the cells intact without being reduced already in the extracellular milieu of cultured cells. Our findings also demonstrate that the impact of **2** on the cell cycle and the nature of cell death resembles that of the parental cisplatin, supporting the view that the **2** acts via an overall mechanism similar to that of cisplatin. We also explored whether DNA damage caused by the binding of platinum from **2** is involved in the mechanism of its antiproliferative activity and found out that reparable DNA damage by platinum moiety released from **2** significantly contributes to its overall biological activity consistent with the reduction of the substitution-inert **2** by intracellular reductants.

Further studies were aimed at demonstrating whether the overall mechanism of antiproliferative activity of **2** also involved the effects of two important functionalities of lonidamine, which affect metabolic processes in cancer cells, namely the inhibition of glycolysis and the reduction of cellular levels of GSH. The results indicated that these important functionalities of lonidamine were unlikely to substantially contribute to the overall antiproliferative activity of **2** via their inherent biological activity. Thus, it is reasonable to conclude that the effect of lonidamine ligands in **2** consists predominantly in the enhancement of lipophilicity of **2,** resulting in the increase of accumulation of DNA damaging Pt moiety in cancer cells.

The low potency of lonidamine ligands in **2** to affect metabolic processes in cancer cells, which free lonidamine is able to affect very efficiently, deserves further discussion. Anticancer Pt(IV) prodrugs containing biologically active axial ligands are known to be reduced by intracellular reductants upon entry into cancer cells. This reduction leads to the simultaneous release of the antitumor Pt(II) complex and molecules of the biologically active substance, which synergistically potentiate the antiproliferative effects of the Pt(II) complex. Another factor that significantly contributes to the higher antiproliferative efficacy of Pt(IV) prodrugs compared to parental Pt(II) complexes is that biologically active axial ligands increase substantially the hydrophobicity of the Pt(IV) complex and thus its accumulation in cancer cells. Thus, it is possible that, in the case of treatment of cancer cells with **2**, the concentration of antitumor Pt (II) complex in the treated cells is markedly increased compared to the situation where cancer cells are subjected to the significantly more hydrophilic parental Pt(II) complex under the same conditions. At the same time, however, the concentration of lonidamine molecules released in cancer cells may be insufficient to manifest the effect of lonidamine on metabolic processes in cancer cells.

Conclusively, the results of this study show that the task of Pt(IV) complex **2** used as a prodrug is to deliver the cytotoxic Pt(II) drug to the cancer cells predominantly and should consider **2** not as a dual- or multi-action prodrug but as the prodrug that effectively delivers cytotoxic Pt(II) complex, rather than lonidamine, to the tumor.

Experimental

The chemicals and instruments

Reagents were purchased from Aldrich unless specified otherwise. All solvents were purified and degassed prior to use. NMR spectra were recorded on a Bruker FT-NMR Avance III 500 MHz

instrument at 500.32 (1H). Chemical shifts were referenced relative to the solvent signal for 1H. ESI mass spectra were recorded on an LC/MSn ion trap mass spectrometer amaZon SL (Bruker, Bremen, Germany) with MeOH as a solvent. Elemental analysis was performed at Moscow State University with MicroCube Elementar analyzer.

Material and cell lines for biological studies

Cisplatin, N,N-dimethylformamide (DMF), and dimethylsulfoxide (DMSO) were from Sigma–Aldrich (Prague, Czech Republic). MTT and neutral red (NR) were from Calbiochem (Darmstadt, Germany) and Sigma Aldrich, Prague, Czech Republic), respectively. Stock solutions for cellular studies were prepared by dissolving Pt compounds or lonidamine in DMF to a final concentration of 5 or 20 mM, respectively, and serially diluted before testing in cell culture media. To avoid DMF toxicity, the final DMF concentration in the cell culture medium did not exceed 1% v/v.

The human breast cancer MCF-7 cells and human colorectal carcinoma cells HCT 116 were kindly supplied by Professor B. Keppler, University of Vienna (Austria). Highly invasive breast carcinoma MDA-MB-231 cells and human MRC-5 pd30 cells derived from normal lung tissue were purchased from the European collection of authenticated cell cultures (ECACC; Salisbury, UK). Chinese hamster ovary CHO-K1 cell line (wild-type) and its derivative MMC-2 carrying the ERCC3/XPB mutation (NER-deficient) cell line were kindly supplied by Dr. M. Pirsel, Cancer Research Institute, Slovak Academy of Sciences, Bratislava (Slovakia). The MCF-7, HCT-116, MDA-MB-231, MRC-5 pd30, CHO-K1, and MMC-2 cells were grown in DMEM medium (Dulbecco's Modified Eagle's Medium, high glucose (4.5 gL^{-1}, PAA) supplemented with gentamycin (50 $mgmL^{-1}$, Serva) and 10 % heat-inactivated fetal bovine serum (PAA, Pasching, Austria). The medium for MRC-5 pd30 was further fortified by 1% non-essential amino acids (Sigma–Aldrich, Prague, CzechRepublic). The cells were cultured in an incubator at 37 °C in a humidified 5 % CO_2 atmosphere and subcultured 2–3 times a week.

In vitro antiproliferative assays

The effect of the investigated compounds on cell proliferation was evaluated using a common MTT assay or, alternatively, by neutral red (NR) assay. The cells were seeded in 96-well tissue culture plates at a density of $2x10^3$ (MCF-7), $4x10^3$ (MDA-MB-231 and HCT-116), $1x10^4$ (MRC-5pd30), and $3x10^3$ (CHO-K1 and MMC-2) cells/well in 100 µL of the medium. After overnight incubation at 37 °C, the cells were treated with the tested compounds in the concentration range of 0 to 50 µM or 0 to 100 µM for **2** or cisplatin, respectively, in a final volume of 200 µL/well for 72 h. As for the MTT assay, 20 µL of a freshly diluted MTT solution (1.25 $mgmL^{-1}$ in PBS) was added to each well after the treatment period, and the plates were incubated at 37 °C in a humidified atmosphere for 3 h. Afterward, the medium was removed, and the resulting formazan product was dissolved in 100 µL of DMSO. The number of living cells in each well was evaluated by measuring the absorbance at 570 nm (reference 620 nm) using the Spark® multimode microplate reader (Tecan, Raleigh, US). For the NR assay, 20 µL of a 0.33% solution of NR in PBS was added to each well after the treatment period, and the cells were incubated at 37 °C for 3 h. Then, the dye-containing medium was thoroughly removed, and the cells were quickly rinsed twice with PBS. Then, the incorporated dye was solubilized in 200 µL of 1% acetic acid in 50% ethanol. The absorbance was measured at 540 nm (reference wavelength at 690 nm). In both assays, the reading values were converted to the percentage of control. Antiproliferative effects were expressed as IC_{50} values calculated from the curves constructed by plotting cell survival (%) versus drug concentration. All experiments were independently repeated at least three times, each repetition made in duplicate.

Toxic effects of the investigated compounds were also determined in 3D cultures of MCF-7 cells. The cells were seeded in ultra-low attachment 96-well plates at a density of 600 cells/well in the growth medium [DMEM; B-27 supplement (1V), EGF (epidermal growth factor, 20 $ngmL^{-1}$) and BSA (1.5 $mgmL^{-1}$)] and allowed to grow for four days. The resulting 96 h-old spheroids were treated with the investigated compounds for an additional 72 h. The CellTiter-Glo 3D cell

viability assay (Promega, Prague, Czech Republic) was used to determine IC_{50} values according to the manufacturer's protocol.

Cellular accumulation

Cellular accumulation of platinum from **2** and cisplatin was determined as already described.[66] In brief, MCF-7 cells were seeded in 10 cm Petri dishes and kept in a drug-free medium at 37 °C in a 5 % CO_2 humidified atmosphere overnight. Then, the cells were treated with compounds at their 10 μM concentrations in the cell growth medium when confluency reached about 80% and allowed drug exposure for 6 h. The cells were subsequently detached using 0.25 % trypsin, washed 3-times carefully with ice-cold PBS, collected by centrifugation, and counted. The cell pellets were digested with concentrated HNO_3, and the quantity of metals taken up by the cells was determined by ICP-OES.

Cell cycle

MCF-7 cells were seeded in 6-well plates at a density of 2×10^5 cells per well. After attaching for 12 h, cells were treated with cisplatin and **2** at different concentrations for 24 h. Cells were harvested by trypsinization, followed by washing three times with ice-cold PBS and fixed in 5 mL of cold 70% ethanol at -20 °C overnight. Before analysis, cells were spun down, washed twice again with PBS, and stained with PI solution (20 μgmL^{-1}, containing 0.1% Triton X-100 and 200 μgmL^{-1} RNase A, pH 7.4) for 15 min at 37 ºC. Samples were finally analyzed by flow cytometer (BD FACS Calibur).

Cell death

MCF-7 cells were seeded in 6-well plates at a density of 2.5×10^5 cells per well and allowed to attach for 12 h. Medium containing cisplatin and **2** was added to the cells at different concentrations. After 12 h treatment, cells were collected by trypsinization and washed twice in PBS. Then the cell pellets were washed once and resuspended in Annexin-V binding buffer at the density of 1×10^6 cells per mL for staining. A volume of 5 μL of FITC Annexin-V and 1 μL of the PI solution was added according to the manufacturer's protocol. The samples were analyzed by a flow cytometer (BD FACS Calibur) after 15 min staining at r.t.

Intracellular DNA platination

Cellular accumulation of the investigated complexes was determined in MCF-7 cells. Briefly, the cells were seeded on 100 mm Petri dishes with a plating density of $7x10^5$ cells/dish. After overnight pre-incubation in a drug-free medium at 37 °C in 5% CO_2, the cells were treated with platinum compounds (0.25 μM) and allowed 24 h of drug exposure. After the treatment, the cells were extensively washed with PBS (37 °C), detached by 0.25% trypsin, and washed twice with ice-cold PBS. The cell pellets were then lysed in DNAzol (DNAzol, MRC) supplemented with RNase A (100 μgmL^{-1}). Genomic DNA was precipitated from the lysate with 100%ethanol, washed twice with 75% ethanol, and resuspended in water. The DNA content in each sample was determined by UV spectrophotometry. To avoid the affection of high DNA concentration and related viscosity on detection of platinum in the samples, the DNA samples were digested in the presence of 30% hydrochloric acid (Suprapur, Merck Millipore). The amount of metal bound to DNA was quantified by ICP-MS. All experiments were performed in triplicate.

Glucose consumption by cells

MCF-7 cells were seeded on 24-well plates (8×10^4 cells/600 μL/well) and grown overnight. The medium was then changed, and the cells were treated with **2**, lonidamine, or cisplatin diluted in the media (400 μL) or left untreated and grown for an additional 24 h. Subsequently, an aliquot of the medium was withdrawn from the wells, and the cells were trypsinized, harvested, and counted. The glucose concentration in the medium was determined using the Amplex® Red Glucose/Glucose Oxidase Assay Kit (Life Technologies) following the manufacturer's protocol.

The glucose accumulation in cells was calculated as the difference between the glucose concentration in the samples and glucose concentration in the cell-free medium and normalized to the number of cells in each sample. It was verified that under the experimental conditions, the viability of cells after the treatment was at least 93%.

Lactate production in cells

MCF-7 cells were seeded in 24-well culture plates at a density of 2.5×10^4/well. After overnight incubation in the complete growth medium, the medium was removed, and cells were washed twice with PBS. Afterward, 400 μL of a serum-free medium without Phenol Red was added to the cells, either drug-free or containing **2**, lonidamine, or cisplatin at a final, roughly equitoxic concentrations corresponding to 2-fold, 3-fold, or 5-fold of the IC_{50}. After 6-h treatment, the plates were spun down at 1000 rpm for 5 min to pellet the insoluble material. The cell culture medium from each sample (150 μL) was withdrawn and loaded into a 10 kDa cutoff spin filter column and spun down at 12 000 rpm for 10 min to remove lactate dehydrogenase. Eluents (4 μL) were added to a 96-well culture plate, and lactate concentration was measured using an enzymatic colorimetric Lactate Assay Kit (Sigma-Aldrich) according to the manufacturer's protocol. The amount of lactate present in the samples was determined from a standard curve plotted for the lactate standards supplied in the kit. The experiments were performed in triplicate. It was verified that under the experimental conditions, the viability of cells after the treatment was at least 95%.

Glycostress test

MCF-7 cells were seeded at a density of 20,000 cells/well and incubated for 24 h at 37 °C, 5% CO_2 in 100 μL DMEM supplemented with 10% FBS in a Seahorse XF 96-well cell culture microplate (Agilent). Cells were then washed with Seahorse XF DMEM medium (Agilent) and incubated for 1 h at 37 °C, 5% CO_2 prior to the assay. 18 min after the start of the assay, **2** (final concentration: 50 μM), cisplatin (final concentration: 50 μM), lonidamine (final concentration: 100 μM), or the vehicle (DMSO) for untreated cells were injected into the wells (8 replicate wells). The assay was then performed according to the manufacturer's instructions using a Seahorse XFe96 Analyzer (Agilent).

Quantification of intracellular glutathione

The intracellular level of GSH was quantified by using GSH-selective cell-permeant probe monochlorobimane. This probe is essentially non-fluorescent until it reacts with glutathione. For this assay, MCF7 cells were seeded on the 6w plates at the density of $2\cdot10^5$ cells/well. After the overnight incubation, the cells were treated with tested compounds at their equitoxic concentrations corresponding to 1, 3, 5 x$IC_{50,72h}$ and cultured for a further 24, 48, and 72 h. Then, samples were harvested and stained with 100 μM of monochlorobimane for 30 min at 37°C. Samples were washed with DPBS, and the fluorescence associated with the cells was analyzed using the flow cytometer CellStream (Luminex, USA). Samples were excited at 405 nm, and the emission was detected on the channel 456/51 nm. The only population of single cells was included in the analysis; debris and other particles were gated out of the analysis. The data were processed by using Luminex analysis software.

In vivo acute toxicity

The Balb/c female mice (8-10 weeks old, weight 20-22 g) were bred and hosted at the animal facility of Blokhin Cancer Center. Mice were kept at 21±1ºC, 50-60% humidity; food and water were added ad libitum. All manipulations were performed in accordance with the European Convention for the Protection of Vertebrate Animals used for Experimental and other Scientific Purposes (ETS 123). Compound **2** was injected i.p.; 70-125 mg/kg single bolus administration in 200 μl saline. Each cohort contained six mice. Animals were monitored for 21 days after injection.

General behavioural activity, nutritional habits, and hair cover integrity were the criteria of acute toxicity.

Biodistribution experiments

Compound 2 was injected i.p. (75 mg/kg) into three 10-week-old male Balb/c mice (weight ~20 g). Animals were sacrificed at 24 h after injection; blood and organ samples were collected for quantitative measurements of Pt content.

ICP-MS sample preparation and measurement

Sample digestion was performed using batches of 8 samples, 100 mg each. Each batch contained 2 control samples. Specimens were placed in one-chamber autoclaves to which 1.0 mL of concentrated HNO_3 (65%, max. 0.0000005% Hg, GR, ISO, Merck) and 0.1 mL of HCl (37%; max. 0.0000005 % Hg; PA-ACS-ISO; Panreac, Spain) were added. The chambers were closed with caps and evacuated in the autoclave titanium housings. The autoclaves were placed in an electric furnace and incubated at 160 °C for 1 h and 180 °C for another 1 h. After cooling, the solutions were diluted with water to 10 mL and transferred to plastic bottles. The same procedure was performed in autoclaves without samples, and the resulting solutions were used as control samples. The Pt content was determined by inductively coupled plasma mass spectrometry (ICP-MS) using an X-II spectrometer (Thermo Scientific, USA) and the following parameters: RF generator power 1400 W, nebulizer PolyCon, spray chamber cooling 3ºC, plasma gas flow rate 12 L/min, auxiliary flow rate 0.9 L/min, nebulizer flow rate 0.9 L/min, sample update 0.8 mL/min, resolution 0.8M. The main parameters of MS measurements were: detector mode double (pulse counting and analogous) and scanning mode Survey Scan and Peak Jumping. The settings for the Survey Scan were: number of runs 10, dwell time 0.6 ms, channels per mass 10, acquisition 13.2 sec. The settings for the Peak Jumping were: sweeps 25, dwell time 10 ms, channels per mass 1, acquisition 34 sec.

Acknowledgments

This work was supported by the Czech Science Foundation (Grant no. 20-14082J) and Russian Foundation for Basic Research (Grant No. 19-53-26002). This work was also financially supported by an ERC Consolidator Grant (PhotoMedMet) to G.G. (GA 681679) and by a Qlife prématuration funding (G.G. and R.V.).

Data availability statement

The datasets generated during and/or analysed during the current study are available from the corresponding author on reasonable request.

References

1 Wang, D. and Lippard, S.J., Cellular processing of platinum anticancer drugs. *Nat. Rev. Drug Discov.*, 2005, 4, 307-320.

2 Kelland, L., The resurgence of platinum-based cancer chemotherapy. *Nat. Rev. Cancer*, 2007, 7, 573-584.

3 Keefe, A.D., Pai, S. and Ellington, A., Aptamers as therapeutics. *Nat. Rev. Drug Discov.*, 2010, 9, 537-550.

4 Florea, A.-M. and Büsselberg, D., Cisplatin as an anti-tumor drug: Cellular mechanisms of activity, drug resistance and induced side effects. *Cancers*, 2011, 3, 1351-1371.

5 Fuertes, M.A., Alonso, C. and Perez, J.M., Biochemical modulation of cisplatin mechanisms of action: Enhancement of antitumor activity and circumvention of drug resistance. *Chem. Rev.*, 2003, 103, 645-662.

6 Brabec, V. and Kasparkova, J. Role of DNA repair in antitumor effects of platinum drugs. In Hadjiliadis, N. and Sletten, E. (eds.), Metal Complex - DNA Interactions, 2009, Wiley, Chichester, UK, 175-208.

7 Todd, R.C. and Lippard, S.J., Consequences of cisplatin binding on nucleosome structure and dynamics. *Chem. Biol.*, 2010, 17, 1334-43.
8 Wu, B., Davey, G.E., Nazarov, A.A., Dyson, P.J. and Davey, C.A., Specific DNA structural attributes modulate platinum anticancer drug site selection and cross-link generation. *Nucleic Acids Res.*, 2011, 39, 8200-8212.
9 Brabec, V., Hrabina, O. and Kasparkova, J., Cytotoxic platinum coordination compounds. DNA binding agents. *Coord. Chem. Rev.*, 2017, 351, 2-31.
10 Johansson, K., Ito, M., Schophuizen, C.M.S., Mathew Thengumtharayil, S., Heuser, V.D., Zhang, J., Shimoji, M., Vahter, M., Ang, W.H., Dyson, P.J., Shibata, A., Shuto, S., Ito, Y., Abe, H. and Morgenstern, R., Characterization of New Potential Anticancer Drugs Designed To Overcome Glutathione Transferase Mediated Resistance. *Mol. Pharm.*, 2011, 8, 1698-1708.
11 Gibson, D., Platinum(IV) anticancer prodrugs - hypotheses and facts. *Dalton Trans.*, 2016, 45, 12983-12991.
12 Johnstone, T.C., Suntharalingam, K. and Lippard, S.J., The Next Generation of Platinum Drugs: Targeted Pt(II) Agents, Nanoparticle Delivery, and Pt(IV) Prodrugs. *Chem. Rev.*, 2016, 116, 3436-3486.
13 Gibson, D., Multi-action Pt(IV) anticancer agents; do we understand how they work? *J. Inorg. Biochem.*, 2019, 191, 77-84.
14 Lee, K.G.Z., Babak, M.V., Weiss, A., Dyson, P.J., Nowak-Sliwinska, P., Montagner, D. and Ang, W.H., Development of an Efficient Dual-Action GST-Inhibiting Anticancer Platinum(IV) Prodrug. *ChemMedChem*, 2018, 13, 1210-1217.
15 Ang, W.H., Khalaila, I., Allardyce, C.S., Juillerat-Jeanneret, L. and Dyson, P.J., Rational Design of Platinum(IV) Compounds to Overcome Glutathione-S-Transferase Mediated Drug Resistance. *J. Am. Chem. Soc.*, 2005, 127, 1382-1383.
16 Dhar, S., Daniel, W.L., Giljohann, D.A., Mirkin, C.A. and Lippard, S.J., Polyvalent oligonucleotide gold nanoparticle conjugates as delivery vehicles for platinum(IV) warheads. *J. Am. Chem. Soc.*, 2009, 131, 14652-14653.
17 Pathak, R.K., Marrache, S., Choi, J.H., Berding, T.B. and Dhar, S., The Prodrug Platin-A: Simultaneous Release of Cisplatin and Aspirin. *Angew. Chem., Int. Ed.*, 2014, 53, 1963-1967.
18 Kenny, R.G. and Marmion, C.J., Toward multi-targeted platinum and ruthenium drugs—A new paradigm in cancer drug treatment regimens? *Chem. Rev.*, 2019, 119, 1058-1137.
19 Wang, Z., Deng, Z. and Zhu, G., Emerging platinum(iv) prodrugs to combat cisplatin resistance: from isolated cancer cells to tumor microenvironment. *Dalton Trans.*, 2019, 48, 2536-2544.
20 Tang, L., Cai, D., Qin, M., Lu, S., Hu, M.-H., Ruan, S., Jin, G. and Wang, Z., Oxaliplatin-Based Platinum(IV) Prodrug Bearing Toll-like Receptor 7 Agonist for Enhanced Immunochemotherapy. *ACS Omega*, 2020, 5, 726-734.
21 Babu, T., Sarkar, A., Karmakar, S., Schmidt, C. and Gibson, D., Multiaction Pt(IV) Carbamate Complexes Can Codeliver Pt(II) Drugs and Amine Containing Bioactive Molecules. *Inorg. Chem.*, 2020, 59, 5182-5193.
22 Muhammad, N., Tan, C.-P., Muhammad, K., Wang, J., Sadia, N., Pan, Z.-Y., Ji, L.-N. and Mao, Z.-W., Mitochondria-targeting monofunctional platinum(II)-lonidamine conjugates for cancer cell de-energization. *Inorg. Chem. Front.*, 2020, 7, 4010-4019.
23 Karges, J., Yempala, T., Tharaud, M., Gibson, D. and Gasser, G., A Multi-action and Multi-target RuII–PtIV Conjugate Combining Cancer-Activated Chemotherapy and Photodynamic Therapy to Overcome Drug Resistant Cancers. *Angew. Chem., Int. Ed.*, 2020, 59, 7069-7075.
24 Fronik, P., Poetsch, I., Kastner, A., Mendrina, T., Hager, S., Hohenwallner, K., Schueffl, H., Herndler-Brandstetter, D., Koellensperger, G., Rampler, E., Kopecka, J., Riganti, C., Berger, W., Keppler, B.K., Heffeter, P. and Kowol, C.R., Structure–Activity Relationships of Triple-Action Platinum(IV) Prodrugs with Albumin-Binding Properties and Immunomodulating Ligands. *J. Med. Chem.*, 2021, 64, 12132-12151.
25 Alessio, M., Zanellato, I., Bonarrigo, I., Gabano, E., Ravera, M. and Osella, D., Antiproliferative activity of Pt(IV)-bis(carboxylato) conjugates on malignant pleural mesothelioma cells. *J. Inorg. Biochem.*, 2013, 129, 52-57.
26 Gabano, E., Ravera, M. and Osella, D., Pros and cons of bifunctional platinum(IV) antitumor prodrugs: two are (not always) better than one. *Dalton Trans.*, 2014, 43, 9813-9820.

27 Schmidt, C., Babu, T., Kostrhunova, H., Timm, A., Basu, U., Ott, I., Gandin, V., Brabec, V. and Gibson, D., Are Pt(IV) prodrugs that release combretastatin A4 true multi-action prodrugs? *J. Med. Chem.*, 2021, 64, 11364-11378.
28 Cervantes-Madrid, D., Romero, Y. and Dueñas-González, A., Reviving lonidamine and 6-diazo-5-oxo-L-norleucine to be used in combination for metabolic cancer therapy. *Biomed Res. Int.*, 2015, 2015, 690492.
29 Nath, K., Guo, L., Nancolas, B., Nelson, D.S., Shestov, A.A., Lee, S.-C., Roman, J., Zhou, R., Leeper, D.B., Halestrap, A.P., Blair, I.A. and Glickson, J.D., Mechanism of antineoplastic activity of lonidamine. *Biochim. Biophys. Acta, Rev. Cancer*, 2016, 1866, 151-162.
30 Shang, C., Hou, Y., Meng, T., Shi, M. and Cui, G., The Anticancer Activity of Indazole Compounds: A Mini Review. *Curr. Top. Med. Chem. (Sharjah, United Arab Emirates)*, 2021, 21, 363-376.
31 Di Cosimo, S., Ferretti, G., Papaldo, P., Carlini, P., Fabi, A. and Cognetti, F., Lonidamine: efficacy and safety in clinical trials for the treatment of solid tumors. *Drugs Today*, 2003, 39, 157-173.
32 Gridelli, C., De Marinis, F., Rossi, A., Tucci, E., D'Aprile, M., Cioffi, R., Cortesi, E., Migliorino, R., Pisano, A., Scognamiglio, F., Di Giacomo, R. and Bianco, A.R., A phase II study of VM-26 plus lonidamine in pretreated small cell lung cancer. *Anticancer Res.*, 1997, 17, 1277-9.
33 Pacini, P., Rinaldini, M., Algeri, R., Guarneri, A., Tucci, E., Barsanti, G., Neri, B., Bastiani, P., Marzano, S. and Fallai, C., FEC (5-fluorouracil, epidoxorubicin and cyclophosphamide) versus EM (epidoxorubicin and mitomycin-C) with or without lonidamine as first-line treatment for advanced breast cancer. A multicentric randomized study. Final results. *Eur. J. Cancer*, 2000, 36, 966-975.
34 Huang, Y., Sun, G., Sun, X., Li, F., Zhao, L., Zhong, R. and Peng, Y., The potential of lonidamine in combination with chemotherapy and physical therapy in cancer treatment. *Cancers*, 2020, 12, 3332.
35 Shutkov, I.A., Okulova, Y.N., Tyurin, V.Y., Sokolova, E.V., Babkov, D.A., Spasov, A.A., Gracheva, Y.A., Schmidt, C., Kirsanov, K.I., Shtil, A.A., Redkozubova, O.M., Shevtsova, E.F., Milaeva, E.R., Ott, I. and Nazarov, A.A., Ru(III) Complexes with Lonidamine-Modified Ligands. *International Journal of Molecular Sciences*, 2021, 22, 13468.
36 Chen, H., Chen, F., Hu, W. and Gou, S., Effective platinum(IV) prodrugs conjugated with lonidamine as a functional group working on the mitochondria. *J. Inorg. Biochem.*, 2018, 180, 119-128.
37 Muhammad, N., Tan, C.-P., Nawaz, U., Wang, J., Wang, F.-X., Nasreen, S., Ji, L.-N. and Mao, Z.-W., Multiaction Platinum(IV) Prodrug Containing Thymidylate Synthase Inhibitor and Metabolic Modifier against Triple-Negative Breast Cancer. *Inorg. Chem.*, 2020, 59, 12632-12642.
38 Nazarov, A.A., Gardini, D., Baquié, M., Juillerat-Jeanneret, L., Serkova, T.P., Shevtsova, E.P., Scopelliti, R. and Dyson, P.J., Organometallic anticancer agents that interfere with cellular energy processes: a subtle approach to inducing cancer cell death. *Dalton Trans.*, 2013, 42, 2347-2350.
39 Nosova, Y.N., Foteeva, L.S., Zenin, I.V., Fetisov, T.I., Kirsanov, K.I., Yakubovskaya, M.G., Antonenko, T.A., Tafeenko, V.A., Aslanov, L.A., Lobas, A.A., Gorshkov, M.V., Galanski, M., Keppler, B.K., Timerbaev, A.R., Milaeva, E.R. and Nazarov, A.A., Enhancing the Cytotoxic Activity of Anticancer PtIV Complexes by Introduction of Lonidamine as an Axial Ligand. *Eur. J. Inorg. Chem.*, 2017, 2017, 1785-1791.
40 Okulova, Y.N., Zenin, I.V., Shutkov, I.A., Kirsanov, K.I., Kovaleva, O.N., Lesovaya, E.A., Fetisov, T.I., Milaeva, E.R. and Nazarov, A.A., Antiproliferative activity of Pt(IV) complexes with lonidamine and bexarotene ligands attached via succinate-ethylenediamine linker. *Inorg. Chim. Acta*, 2019, 495, 119010.
41 Duan, J.-X., Method for synthesis of lonidamine and related indazole derivatives. *WO 2005/120498 A2*, 2005.
42 Berridge, M.V. and Tan, A.S., Characterization of the Cellular Reduction of 3-(4,5-dimethylthiazol-2-yl)-2,5-diphenyltetrazolium bromide (MTT): Subcellular Localization, Substrate Dependence, and Involvement of Mitochondrial Electron Transport in MTT Reduction. *Arch. Biochem. Biophys.*, 1993, 303, 474-482.
43 Brawer, M.K., Lonidamine: basic science and rationale for treatment of prostatic proliferative disorders. *Rev. Urol.*, 2005, 7, S21-S26.
44 Repetto, G., del Peso, A. and Zurita, J.L., Neutral red uptake assay for the estimation of cell viability/cytotoxicity. *Nat. Protoc.*, 2008, 3, 1125-1131.

45 Zanoni, M., Piccinini, F., Arienti, C., Zamagni, A., Santi, S., Polico, R., Bevilacqua, A. and Tesei, A., 3D tumor spheroid models for in vitro therapeutic screening: a systematic approach to enhance the biological relevance of data obtained. *Sci. Rep.*, 2016, 6, 19103.
46 Thoma, C.R., Zimmermann, M., Agarkova, I., Kelm, J.M. and Krek, W., 3D cell culture systems modeling tumor growth determinants in cancer target discovery. *Adv. Drug Delivery Rev.*, 2014, 69-70, 29-41.
47 Wernitznig, D., Kiakos, K., Del Favero, G., Harrer, N., Machat, H., Osswald, A., Jakupec, M.A., Wernitznig, A., Sommergruber, W. and Keppler, B.K., First-in-class ruthenium anticancer drug (KP1339/IT-139) induces an immunogenic cell death signature in colorectal spheroids in vitro. *Metallomics*, 2019, 11, 1044-1048.
48 Baker, B.M. and Chen, C.S., Deconstructing the third dimension – how 3D culture microenvironments alter cellular cues. *J. Cell Sci.*, 2012, 125, 3015-3024.
49 Wartenberg, M., Ling, F.C., Müschen, M., Klein, F., Acker, H., Gassmann, M., Petrat, K., Pütz, V., Hescheler, J. and Sauer, H., Regulation of the multidrug resistance transporter P-glycoprotein in multicellular tumor spheroids by hypoxia-inducible factor (HIF-1) and reactive oxygen species. *FASEB J.*, 2003, 17, 503-505.
50 Minchinton, A.I. and Tannock, I.F., Drug penetration in solid tumours. *Nat. Rev. Cancer*, 2006, 6, 583.
51 Kimlin, L.C., Casagrande, G. and Virador, V.M., In vitro three-dimensional (3D) models in cancer research: An update. *Mol. Carcinog.*, 2013, 52, 167-182.
52 Ravi, M., Paramesh, V., Kaviya, S.R., Anuradha, E. and Solomon, F.D.P., 3D cell culture systems: Advantages and applications. *J. Cell. Physiol.*, 2015, 230, 16-26.
53 Pulze, L., Congiu, T., Brevini, T.A.L., Grimaldi, A., Tettamanti, G., D'Antona, P., Baranzini, N., Acquati, F., Ferraro, F. and de Eguileor, M., MCF7 Spheroid Development: New Insight about Spatio/Temporal Arrangements of TNTs, Amyloid Fibrils, Cell Connections, and Cellular Bridges. *Int. J. Chem. Sc.*, 2020, 21.
54 Karmakar, S., Kostrhunova, H., Ctvrtlikova, T., Novohradsky, V., Gibson, D. and Brabec, V., Platinum(IV)-estramustine multiaction prodrugs are effective antiproliferative agents against prostate cancer cells. *J. Med. Chem.*, 2020, 63, 13861-13877.
55 Göschl, S., Varbanov, H.P., Theiner, S., Jakupec, M.A., Galanski, M. and Keppler, B.K., The role of the equatorial ligands for the redox behavior, mode of cellular accumulation and cytotoxicity of platinum(IV) prodrugs. *J. Inorg. Biochem.*, 2016, 160, 264-274.
56 Kostrhunova, H., Petruzzella, E., Gibson, D., Kasparkova, J. and Brabec, V., A new anticancer Pt(IV) prodrug that acts by mechanisms involving DNA damage and different epigenetic effects. *Chem. - Eur. J.*, 2019, 25, 5235 – 5245.
57 Eastman, A., Improving anticancer drug development begins with cell culture: misinformation perpetrated by the misuse of cytotoxicity assays. *Oncotarget*, 2017, 8, 8854-8866.
58 Kasparkova, J., Kostrhunova, H., Novakova, O., Křikavová, R., Vančo, J., Trávníček, Z. and Brabec, V., A photoactivatable platinum(IV) complex targeting genomic DNA and histone deacetylases. *Angew. Chem., Int. Ed.*, 2015, 54, 14478-14482.
59 Kasparkova, J., Novakova, O., Vrana, O., Intini, F., Natile, G. and Brabec, V., Molecular aspects of antitumor effects of a new platinum(IV) drug. *Mol. Pharmacol.*, 2006, 70, 1708-1719.
60 Novohradsky, V., Zerzankova, L., Stepankova, J., Vrana, O., Raveendran, R., Gibson, D., Kasparkova, J. and Brabec, V., Antitumor platinum(IV) derivatives of oxaliplatin with axial valproato ligands. *J. Inorg. Biochem.*, 2014, 140, 72-79.
61 Novohradsky, V., Zanellato, I., Marzano, C., Pracharova, J., Kasparkova, J., Gibson, D., Gandin, V., Osella, D. and Brabec, V., Epigenetic and antitumor effects of platinum(IV)-octanoato conjugates. *Sci. Rep.*, 2017, 7, 3751.
62 Zajac, J., Novohradsky, V., Markova, L., Brabec, V. and Kasparkova, J., Platinum(IV) derivatives with cinnamate axial ligands are potent agents against both differentiated and tumorigenic cancer stem Rhabdomyosarcoma cells. *Angew. Chem., Int. Ed.*, 2020, 59, 3329-3335.
63 Kostrhunova, H., Zajac, J., Markova, L., Brabec, V. and Kasparkova, J., A multi-action Pt^{IV} conjugate with oleate and cinnamate ligands targets human epithelial growth factor receptor HER2 in aggressive breast cancer cells. *Angew. Chem., Int. Ed.*, 2020, 59, 21157-21162.

64 Jiang, B., Aerobic glycolysis and high level of lactate in cancer metabolism and microenvironment. *Genes Diseases*, 2017, 4, 25-27.
65 Han, Y., Yin, W., Li, J., Zhao, H., Zha, Z., Ke, W., Wang, Y., He, C. and Ge, Z., Intracellular glutathione-depleting polymeric micelles for cisplatin prodrug delivery to overcome cisplatin resistance of cancers. *J. Controlled Release*, 2018, 273, 30-39.
66 Kostrhunova, H., Zajac, J., Novohradsky, V., Kasparkova, J., Malina, J., Aldrich-Wright, J.R., Petruzzella, E., Sirota, R., Gibson, D. and Brabec, V., A subset of new platinum antitumor agents kills cells by a multimodal mechanism of action also involving changes in the organization of the microtubule cytoskeleton. *J. Med. Chem.*, 2019, 62, 5176-5190.

Table 1. IC_{50} mean values (μM) of **2** and cisplatin evaluated using MTT assay in cancer cells[a]

	MCF-7	MDA-MB-231	HCT 116	MRC-5 pd30
2	0.36 ± 0.01	0.281 ± 0.003	0.29 ± 0.01	1.9 ± 0.1
cisplatin	7.2 ± 0.8	22 ± 2	11 ± 2	11 ± 4
lonidamine	118 ± 9	133 ± 7	110 ± 4	>150

[a]The drug-treatment period was 72 h. The results are expressed as mean values ± SD from three independent experiments performed in duplicate.

Table 2. IC_{50} mean values (μM) of **2**, lonidamine, and cisplatin evaluated using MTT and NR assays in MCF-7 cancer cells[a]

	MTT	NR
2	0.36 ± 0.01	0.372 ± 0.006
cisplatin	7.2 ± 0.8	7.8 ± 0.1
lonidamine	118 ± 9	123 ± 8

[a]The drug-treatment period was 72 h. The results are expressed as mean values ± SD from three independent experiments performed in duplicate.

Table 3. IC_{50} values [mean values, μM][a] for **2** and cisplatin in 3D MCF-7 cell culture for a 72 h incubation period determined by using CellTiter-Glo 3D cell viability assay[a]

2	1.6 ± 0.4
cisplatin	18 ± 3

[a]The results are expressed as mean values ± SD from three independent experiments performed in a quadruplicate; the drug-treatment period was 72 h.

Table 4. Cellular platinum accumulation in MCF-7 cells and log *P* (octanol/water) values obtained by the shake flask method

	2	cisplatin
Cellular uptake (μg Pt/10^6 cells)[a]	208 ± 11	20 ± 9
log *P*[b]	1.8[c]	-2.3[d]

[a] MCF-7 cells were treated with 10 μM compounds for 6 h. Results are expressed as the mean values ± SD from four independent experiments in triplicate for each run.
[b] Partition coefficient log *P* (octanol/water).
[c] Taken from Ref. [39]
[d] Taken from Ref. [54]

Table 5. Platinum content of genomic DNA (pg Pt/μg DNA) isolated from MCF-7 cells treated with **2** or cisplatin. IC_{50} values [mean values, μM] for **2** and cisplatin in Chinese hamster ovary CHO-K1 cell line (wild-type) and its mutant cell line MMC-2 deficient in DNA repair as determined by MTT assay.

	DNA platination[a]	CHO-K1[b]	MMC-2[b]
2	15.3 ± 0.8	4.2 ± 0.2	0.447 ± 0.005
cisplatin	1.4 ± 0.2	22 ± 3	2.0 ± 0.1

[a]The cells were treated with platinum compounds at the 0.25 μM concentration for 24 h. Results are expressed as the mean values ± SD from at least three independent experiments in triplicate for each run.
[b]The drug-treatment period was 72 h. The results are expressed as mean values ± SD from three independent experiments, each performed in triplicate.

Table 6 Distribution of compound **2** in mice tissues in ng/organ .

Organ	**24 h**
Liver	394.21
Kidney	69.97
Lung	21.48
Brain	0.37
Blood cell fraction	8.15
Plasma	4.93